Assessment of lime-cement mortar microstructure and properties by P- and S- ultrasonic waves

I. Palomar[1], G. Barluenga

Department of Architecture, University of Alcala, Madrid, Spain

ABSTRACT

Lime-cement mortars are used for repairing building walls, improving thermal and acoustic performance through the modification of their composition and, consequently, their microstructure and properties. In order to evaluate the applicability of ultrasonic (US) waves to better understand the relationships among composition-microstructure-properties, an experimental program using transmission P- and S- waves was carried out. The properties of ten mortars were assessed by US parameters as velocity, moduli and attenuation coefficient. Water to binder ratio, porosity and thermal conductivity showed good correlation to US modulus while S-wave attenuation was linked to sound absorption and the incorporation of fibres. Flexural strength correlated to P-wave attenuation, while a combination of S-wave attenuation and moduli was needed to adjust compressive strength. These correlations can be useful tools for predictive models development, composition optimization and US on-site evaluation.

KEYWORDS

Lime-cement mortar; ultrasonic pulse; microstructure; hardened properties.

HIGHLIGHTS

- Lime-cement mortars were characterized by P- and S- ultrasonic waves.
- US raw signals were processed to calculate US velocity, moduli and attenuation.
- Bulk modulus was related to w/b, pore structure and thermal conductivity.
- P-wave attenuation correlated to flexural strength.
- S-wave attenuation identified mortars with and without fibres.

[1] Corresponding author. Departamento de Arquitectura. Escuela de Arquitectura, Universidad de Alcalá, C. Santa Úrsula, 8. Alcalá de Henares, 28801 Madrid, Spain. Tel.: +34 918839239; fax: +34 918839246

E-mail address: irene.palomar@uah.es (I. Palomar)

1. Introduction

Lime-cement mortars are widely used for external rendering of building walls due to their better material compatibility and larger plasticity than cement mortars. When used as repair mortars, some composition modifications can be done to further improve thermal and acoustic properties [1]. This advance can be achieved because the change on mortar composition produces changes on the hardened microstructure that would turn into changes in their properties. Accordingly, some correlations among composition, microstructure and performance parameters have been proposed for those mortars [1]. However, there are still some relations that need to be defined to better understand the effect of mortar composition on microstructure and properties, which will allow to design better repairing mortars [2].

Ultrasonic (US) technique can be used with this aim as an evaluation tool for porous building materials' microstructure characterization and can be tuned up in the laboratory for on-site evaluation [3]. Furthermore, US testing is a quick and inexpensive technique useful to compare different materials [4].

US evaluation is based on stress-wave propagation and several US parameters can be obtained, as ultrasonic pulse velocity (UPV), elasticity moduli and attenuation coefficient. Compression waves (P-wave) are widely used for materials' characterization, whereas shear waves (S-waves) have been less used because they are more difficult to process. Nevertheless, a successful method to define P- and S-wave UPV on cement based materials, using Hilbert transform algorithm, has been proposed [5].

US parameters can be related to cement based materials' properties. Some relations between P-wave UPV and mechanical properties (compressive strength and Young modulus) have been described for different concrete types [6, 7, 8]. Two independent elastic constants (elasticity modulus and Poisson's ratio) can be estimated by measuring the compression and shear (P- and S) UPV [9]. Additionally, UPV is affected by the ultrasonic frequency, especially on dispersive materials as cement based materials [10]. The raw US signal attenuation has also been used for cement mortar and concrete samples characterization [11, 12, 13]. Regarding thermal and acoustic performance, few correlations have been described [14, 15].

US parameters have also been correlated to composition parameters and microstructure of building materials. Spectral analysis was successfully used to identify the water to cement (w/c) ratio in concrete [16]. UPV and attenuation were used to measure the void content and porosity in composite materials [17, 18] and cement mortars [19]. In addition, some correlations among pore structure (porosity and permeability), w/c ratio and ultrasonic parameters have been documented [20]. Alternative research proposed an indirect US method to estimate the pore tortuosity in plastic foam samples [21].

Although UPV, elastic modulus and attenuation are useful US parameters for physical and mechanical characterization, a holistic approach by measuring direct transmission time and attenuation, combining ultrasonic transducers with different frequencies would allow to further evaluate porous materials.

Accordingly, this paper presents an experimental program aimed to assess the properties of ten lime-cement mortars, designed to improve thermal and acoustic behaviour as wall renderings [1, 2], by P- and S- US waves. The purpose of this study was to evaluate the hardened performance of these mortars using a portable US device. US P- and S- waves were analysed to obtain UPV by Hilbert transform algorithm, US moduli, Poisson's ratio and attenuation coefficient (AT). Composition, pore structure, mechanical, thermal and acoustic parameters were considered in order to propose correlations to US parameters. These correlations would be useful for predictive models, optimization and on-site evaluation based on portable US devices.

2. Experimental program

2.1. Materials

The materials used for mortar production are described below:

- The conglomerate was a mixture of a lime class CL 90-S and a white cement BL, type II/B-L 32.5 N, supplied by Readymix-Asland S.A.
- A normal-weight siliceous gap-graded aggregate (2-3 mm) and three lightweight aggregates (LWA): expanded clay (A), perlite (P) and vermiculite (V), were used. The LWA particle size was 4 mm (A) and 0-2 mm (P and V). Fig. 1 presents the particle size distribution of lightweight aggregates, which changed due to mixing process [1].
- A cellulose fibre (FC) of 1 mm length – Fibracel ® BC-1000 (Ø20μm) - supplied by Omya Clariana S.L. and a polypropylene fibre (FPP) of 6 mm length - MASTERFIBER 21 (Ø31-35μm)- supplied by BASF Construction Chemicals España S.L. were also used.

Table 1 summarizes the compositions of the ten lime-cement mortars in this study. The nominal apparent density of the components is also in Table 1.The water to binder ratio (w/b) was adjusted to get a plastic consistency and similar workability for all the fresh samples. Ten mortar compositions (1:1:6 by volume) were prepared as described below:

- A reference lime-white cement mortar (REFC) with siliceous gap-graded aggregate (GGA). The volume of lime-paste did not fill the voids formed by the GGA [1]. In a previous study, REFC was compared to a lime-cement mixture with a continuous siliceous aggregate (0-4). The composition with the gap-graded aggregate (REFC) improved early age behaviour and acoustic performance and did not vary significantly the mechanical performance and workability [1].

- Five mixtures where 25 and 50% of GGA was replaced by three lightweight aggregates (LWA) - expanded clay (A), perlite (P) and vermiculite (V). These mixtures were labelled as A25, P25, P50, V25 and V50. In compositions with vermiculite (V) and perlite (P) aggregates, the fine content increased the paste volume and the volume fraction of voids was lower [1].
- Three mortars with cellulose fibres, 1.5% (FC15) and 3% (FC30 and P25FC30) of the total dried mortar's volume, and another mixture that incorporated 810 g of FPP per cubic meter of dried mortar (P25FPP).

2.2. Experimental methods and previous results

2.2.1. Ultrasonic assessment: UPV, US moduli and attenuation coefficient

Hardened samples (40x40x160 mm) were evaluated with a PUNDIT Lab ® US device using P-wave 54 kHz and P- and S-wave 250 kHz transducers. The amplitudes (A_m) in time domain (μs) of the P- and S-wave raw signal (in Volts) through mortar samples were obtained. In addition, transmission times (t_p and t_s), were identified using the Hilbert transform algorithm [5]. The results were analysed according to the data processing method described in Fig.2. Afterwards, compressive modulus (M), shear modulus (G), bulk modulus (K) dynamic, Young modulus (E) and Poisson's ratio (v) were calculated, according to Eqs. (1), (2), (3), (4) and (5) respectively [9].

$$M = \rho V_P^2 / 10^6 \quad (1)$$

$$G = \rho V_S^2 / 10^6 \quad (2)$$

$$K = \rho \left(V_P^2 - \frac{4}{3} V_S^2 \right) / 10^6 \quad (3)$$

$$E = 2G(1 + v) \quad (4)$$

$$v = (0.5V_P^2 - V_S^2)/(V_P^2 - V_S^2) \quad (5)$$

where ρ is the apparent (bulk) density (g/cm^3) and V_P and V_S are the P- and S-wave velocity (m/s), respectively.

The attenuation coefficients (AT_{FRQ}) for 54 and 250 kHz frequencies were determined considering the amplitude (A_m) of the raw US signal in Volts through the samples and calculated according to Eq. (6) [13]:

$$AT_{FRQ} = -(20/x)(\log(A_m/A_T)) \quad (6)$$

where A_T is the amplitude measured when both transducers (transmitter and receiver) were placed face to face and x is the distance between them in a specific specimen (160 mm). This approach points out that the higher the attenuation coefficient (AT_{FRQ}), the lower the US energy absorbed by the sample.

2.2.2.Lime-cement mortar characterization and properties

The ten lime-cement mortars were characterised in the fresh and hardened state. The fresh mortar consistency was measured using the flow table test, according to the European standard UNE-EN 1015-3, in order to fix the water to binder ratio to obtain a plastic consistency.

In the hardened state, several mechanical and physical parameters were characterised on 40 x 40 x 160 mm prismatic samples. The experimental set-up and test procedures have been previously published in [1]. Apparent density (D) and compressive (f_{cm}) and flexural (f_{ctm}) strength at 28 days were tested complying with UNE-EN 1015-10 and UNE-EN 1015-11. Also, open porosity (P_O - accessible to water), capillary water absorption coefficient (C) and water vapor permeability (P_V -wet condition) were calculated according to the measuring procedure of UNE-EN 1015-10. UNE-EN 1015-18 and UNE-EN 1015-19. Besides, the thermal conductivity (λ) and sound absorption coefficient (α_{NRC}) were calculated according to the method previously described [1] and UNE-EN ISO 10534-2, respectively. Table 2 summarizes the experimental results of the ten mortars considered in the study. Some correlations among the composition parameters and properties have been described in a previous work [1].

3. Experimental results: Ultrasonic pulse parameters characterization and analysis

3.1. Ultrasonic pulse velocity (UPV): P-waves (V_{P-54} and V_{P-250}) and S-waves (V_{S-250})

Table 3 summarizes P- and S-wave velocities at 54 and 250 kHz (V_{P-54}, V_{P-250} and V_{S-250}). It can be observed that V_{P-250} were slightly higher than V_{P-54} for all the mortars, as it was expected [10]. V_{P-54} and V_{P-250} varied between 1900 and 3100 m/s and two groups of mortars were identified: one with UPV values around 2950 ± 150 m/s (REFC, FC15, FC30 and A25) and another with UPV values around 2250 ± 250 m/s. These differences can be explained by the changes in mortar composition due to the addition of GGA, LWA (expanded clay) and cellulose fibers [1]. The consequence of the inclusion of perlite (P) and vermiculite (V) aggregate in the mix increased open porosity and lessened the interconnected solid structure which slowed down UPV [18].

V_{S-250} ranged from 1300 to 1700 m/s, which is around half of V_{P-250} values, that accords to results previously reported [20]. FC15 showed the largest values of V_{P-54}, V_{P-250} and V_{S-250}, whereas V50 exhibited the lowest ones, which corresponded to the one of the lowest open porosity and maximum open porosity respectively. Summarising, FC15 increased UPV values regarding REFC, while decreased in all the other mortars, except for V_{P-54} in A25 mixture. On the other hand, larger amounts of cellulose fibres and LWA reduced UPV.

3.2. Ultrasonic moduli: Compressive moduli (M_{54} and M_{250}), shear modulus (G), bulk modulus (K) and dynamic Young Modulus (E)

Table 3 presents the values of Ultrasonic compressive modulus (M_{54} and M_{250}), UPV shear modulus (G), bulk modulus (K), dynamic Young modulus (E), and Poisson's ratio (v), that were calculated according to Eq. 1, 2, 3, 4 and 5. Compressive modulus -M_{54} and M_{250}- ranged from 5 to 18 GPa although M_{54} was slightly lower than M_{250}, due to the influence of UPV on its calculation (Eq. 1).

Shear modulus (G) went between 2 to 6 GPa, Bulk modulus (K) varied from 3 to 11 GPa and dynamic Young modulus (E) from 4 to 14 GPa. As V_{P-54} and V_{P-250} were the most influential values in M_{54} and M_{250}, the same two groups of mortars were identified. Samples with cellulose fibres (FC15) showed the largest moduli, while compositions with vermiculite (V50) had the lowest values. As expected, Poisson's ratio (v) was around 0.25±0.05.

When the US moduli where compared, it was observed that the compressive modulus (M) and the bulk modulus (K) were directly proportional and the shear modulus (G) and the dynamic Young modulus (E) also showed a highly positive correlation [22].

3.3. Ultrasonic attenuation coefficient (AT_{54} and AT_{250})

Table 3 also records the results of attenuation coefficient (AT_{54} and AT_{250}). AT_{54} varied between 0.160 and 0.280 dB/mm, while AT_{250} ranged from 0.080 to 0.180 dB/mm. As expected, frequency affected attenuation [11, 17] due to the heterogenic nature of lime-cement mortars which behave as dispersive materials [10]. AT_{54} value of REFC was the lowest value (0.169 dB/mm) while P25FC30 showed the largest. The lower volume fraction of voids with LWA and fibres (P25FC30) reduced the P- or compressional ultrasonic wave attenuation.

On the other hand, AT_{250} of mortars with fibers - showed a different trend regarding the mixes with GGA and LWA -. These results agree with the effect of size, shape and distribution of fibers on ultrasonic attenuation pointed out by other authors [23]. In addition, the higher frequency, 250 kHz, is more sensitive than 54 kHz to detect the effect of the components' particle size [24]. Consequently, LWA (particle size under 2mm) reduced AT_{250} value of REFC (particle size 2-3 mm), except A25 (particle size 4 mm).

The increase of LWA volume affected AT_{250}, facilitating US energy transmission through the sample. Mortars with both LWA and short fibers (P25FC30 and P25FPP) significantly increased AT_{250} value regarding to (P25), especially P25FC30. However, adding fibers to REFC (FC15 and FC30) reduced AT_{250} value, because cellulose fibers are more flexible than GGA and absorbed more US energy.

In general, these differences could be explained as the attenuation effect is due to scattering and water absorption [11]. In both attenuation coefficients (AT_{54} and AT_{250}), P25FC30 facilitated US energy transmission since FC would reduce internal losses for P- and S- ultrasonic waves. Regarding mortars which absorbed more energy, the difference can be explain due to the pore structure. Particularly, lower frequency

(AT_{54}) is more affected by lower porosity mixtures (REFC) while the attenuation of higher frequency (AT_{250}) varies on higher porosity mortars (V50).

4. Ultrasonic analysis of mortar composition and properties

The US parameters calculated in the previous section, UPV, moduli of elasticity and attenuation coefficient, can be correlated to the mortar composition and properties. According to the mortar design methodology [1], three groups of mortar parameters were considered: mortar composition, solid microstructure and pore network related properties and thermal and acoustic performance. As far as the compressive modulus (M) and the bulk modulus (K) were directly proportional and the shear modulus (G) and the dynamic Young modulus (E) also showed a highly positive correlation, K were considered in the correlation analysis, except once where E showed a better adjustment.

4.1. US evaluation of mortar composition: water to binder ratio and fibre content

The changes in the mortar composition due to the incorporation of different components (GGA, LWA and fibres) modified the w/b ratio required to achieve a plastic consistency of the mortar in the fresh state. It has been previously reported that w/b ratio has a large influence on early age behaviour and pore structure (open porosity and capillary) [1]. Consequently, w/b can be analysed as a key parameter to describe microstructural changes due to the changes in the composition, which can be assessed by ultrasonic data analysis [16]. Accordingly, an evaluation of w/b by US analysis was carried out and is plotted in Fig. 3. An inverse linear relationship between w/b and bulk modulus (K) was identified and the correlation equation is shown in Fig. 3a. As far as $V_{P\text{-}250}$ and $V_{S\text{-}250}$ are the most influential values in K, it can be said that a larger w/b ratio reduced UPV. On the other hand, the compositions with lower water demand, REFC, FC15, FC30 and A25 (lower w/b) showed a more interconnected solid network which facilitated US waves transmission [9]. The use of perlite and vermiculite (P25, P50, P25FC30, P25FPP, V25, and V50) increased the water demand to get a plastic consistency and similar workability, which affected the microstructure [1] and slowed down both P- and S- wave transmission, reducing K values.

Fig. 3b relates w/b ratio and AT_{250}. Two trends were identified: mortars with fibres (f) showed a high positive correlation, whereas GGA and LWA mortars (a) had a negative correlation. Mortars with fibres and larger amount of paste (larger w/b) absorbed more US energy while LWA increased the water demand, reducing the dynamic Young modulus (E) [7]. These changes in elastic properties can explain those changes in AT_{250} trend which could be a useful tool for identifying mortars with fibres.

4.2. US Assessment of mortar microstructure and related properties

The hardened material microstructure deeply affect the US transmission properties of mortars. The solid structure would facilitate the US wave transmission while the pore network would delay US transmission.

Accordingly, US parameters can be used as indirect measurements of properties related either to the solid structure or the pore network.

4.2.1. Solid structure: density and mechanical properties

Fig. 4 plots two correlations found between mechanical properties and US parameters. Fig. 4a shows an inverse linear relationship between compressive strength (S_{COMP}) and a combination of two US parameters (K and AT_{250}). The dependence of the correlation on AT_{250} produced a different correlation equation for mortars with fibres (f) regarding mortars without fibres (a). The high dependence of S_{COMP} on AT_{250} can be explained because the attenuation of ultrasonic pulse is a combined effect of the geometric dispersion and energy dissipation [11], while the effect of K is related to the solid network interconnection that facilitates the US wave transmission [6].

Fig. 4b shows a direct relationship between flexural strength (S_{FLEX}) and AT_{54} for all compositions, but FC15. The larger the flexural strength, the higher the attenuation coefficient (lower US energy absorbed) of P-wave at 54 kHz. Previously, a correlation between S_{FLEX} and $V_{P\text{-}54}$ was described in the literature [8].

Bulk density (D) could be correlated to a combination of dynamic Young modulus (E) and AT_{250} and is plotted in Fig. 5. A different correlation equation was found again for compositions with fibres (f) regarding mortars with GGA and LWA (a).

4.2.2. Pore network: open porosity, water absorption and vapour permeability

Fig. 6 plots open accessible to water porosity (P_O), capillary water absorption coefficient (C) and water vapour permeability (P_V) against bulk modulus (K) and attenuation (AT_{250}). Negative power adjustments were found between K and P_O (Fig. 6a) and C (Fig. 6c). This coincidence for both parameters K and P_O can be explained based on the relationship between open porosity (P_O) and capillary water absorption coefficient (C) defined in a previous paper [1], because the increase in open porosity of the lime-cement mortars was due to capillary pores, especially in samples with perlite and vermiculite LWA. Furthermore, UPV of both P- and S-wave at 250 kHz were greatly affected by the increase of capillary pore network.

On the other hand, a linear relationship was found for P_V and K and is plotted in Fig. 6e. The different trend for P_V regarding to C can be explained considering the different effect of pore sizes on transport properties of mortars and wave attenuation [26], as the thin capillary pores increase C while reduces P_V.

Fig. 6b and 6d plot some linear correlations between AT_{250} and Po and C, respectively. The different trend for mortars with fibres (f) can be explained considering the linear relationship between w/b and Po and C [1], and the effect of fibre on attenuation.

4.3. Ultrasonic evaluation of thermal and acoustic parameters

Thermal conductivity (λ) and bulk modulus (K) were directly related for samples with GGA and LWA (Fig. 7a), following the relation between P-wave UPV and λ described for cementitious based materials containing LWA [14]. It can be highlighted that thermal conductivity (λ) has been described to be related to density (D) and pore structure, except for samples with fibres [1]. Therefore, a combination of properties related to the solid structure and the pore network govern the thermal performance of these mortars.

On the other hand, when sound absorption coefficient (α_{NRC}) and AT_{250} where correlated, again two different trends were found, as showed in Figure 7b. Mortars with fibres showed a negative correlation, whereas a positive one was found on GGA and LWA compositions. This point could be explained considering the different elastic behaviour of fibres and LWA. In general, large acoustic wave absorption was linked to an extensive network of macro-pores [27], low open porosity and large tortuosity [28]. In addition, indirect methods based on ultrasonic measurements have been used to estimate tortuosity [21]. According to the results on LWA samples, their pore structure hindered the US wave attenuation coefficient. The relation among LWA, open porosity and tortuosity can explain this behaviour as some LWA (perlite and vermiculite) filled the large voids of GGA [1]. On contrast, expanded clay (particle size 4 mm) increased the material's overall tortuosity, improving α_{NRC} [29]. On lime-cement mortar with fibres, the greater the attenuation, the higher the sound acoustic absorption.

5. Conclusions

This paper presents a study aimed to assess the microstructure and properties of lime-cement mortars by ultrasonic (US) P- and S-wave transmission. The experimental program comprised measuring transmission time aided by Hilbert wave transformation method (HT), and calculating US velocity, moduli of elasticity, Poisson's ratio and attenuation coefficient (AT). Those US parameters were correlated to composition parameters (w/b ratio and incorporation of fibres), compressive and flexural strength, bulk density, open porosity (accessible to water), capillary water absorption coefficient, water vapour permeability, thermal conductivity and sound absorption coefficient. These correlations can be useful tools for predictive models development, composition optimization and US on-site evaluation.

The main conclusions of this study were as follows:

- Different trends were described on ultrasonic wave velocity and attenuation due to the use of different components for improving thermal and acoustic performance, as siliceous gap-graded aggregates, lightweight aggregates and short fibres. There was a direct effect of water to binder ratio (w/b ratio) on US parameters such as the bulk modulus (K) and S-wave attenuation (AT_{250}).
- The attenuation of S-waves (AT_{250}) allowed to identify mortars with fibres, especially when pore structure was assessed.

- P-wave attenuation (AT_{54}) and flexural strength (S_{FLEX}) showed a direct relationship. However, more complex relations were necessary for compressive strength (S_{COMP}) and bulk density (D).
- Regarding to the relationships found out between US and pore structure parameters, strong correlations were identified among bulk modulus (K) and open porosity (P_O), capillary water absorption (C) and water vapour permeability (P_V).
- Thermal conductivity (λ) and bulk modulus (K) were linearly related, except for mortars with fibres. On the other hand, sound absorption coefficient (α_{NRC}) was connected to S-wave attenuation (AT_{250}) in a trend that allowed to identify mortars with fibres.

Acknowledgments

The authors wish to acknowledge the financial support for this Research, provided by the Grant for training of Lecturers (FPU-UAH 2013), funded by University of Alcalá. Some of the components were supplied by BASF Construction Chemicals España S.L., Omya Clariana S.L. and Readymix-Asland S.A.

References

[1] I. Palomar, G. Barluenga, J. Puentes, Lime–cement mortars for coating with improved thermal and acoustic performance, Construction and Building Materials, Volume 75, 30 January 2015, Pages 306-314, http://dx.doi.org/10.1016/j.conbuildmat.2014.11.012.

[2] I. Palomar, G. Barluenga, Lime-cement mixture with improved thermal and acoustic characteristics (*Patent in Spanish*), Publication number ES2548221, 2014, Madrid, Spain: OEPM.

[3] A. Moropoulou, K.C. Labropoulos, E.T. Delegou, M. Karoglou, A. Bakolas, Non-destructive techniques as a tool for the protection of built cultural heritage, *Construction and Building Materials*, Volume 48, November 2013, Pages 1222-1239, http://dx.doi.org/10.1016/j.conbuildmat.2013.03.044.

[4] O. Cazalla, E. Sebastián, G. Cultrone, M. Nechar, M.G. Bagur, Three-way ANOVA interaction analysis and ultrasonic testing to evaluate air lime mortars used in cultural heritage conservation projects, *Cement and Concrete Research*, Volume 29, Issue 11, November 1999, Pages 1749-1752, http://dx.doi.org/10.1016/S0008-8846(99)00158-1.

[5] R. Birgül, Hilbert transformation of waveforms to determine shear wave velocity in concrete, *Cement and Concrete Research*, Volume 39, Issue 8, August 2009, Pages 696-700, http://dx.doi.org/10.1016/j.cemconres.2009.05.003.

[6] R. Demirboğa, İ. Türkmen, M.B. Karakoç, Relationship between ultrasonic velocity and compressive strength for high-volume mineral-admixtured concrete, Cement and Concrete Research, Volume 34, Issue 12, December 2004, Pages 2329-2336, http://dx.doi.org/10.1016/j.cemconres.2004.04.017.

[7] J.A. Bogas, M.G. Gomes, A. Gomes, Compressive strength evaluation of structural lightweight concrete by non-destructive ultrasonic pulse velocity method, Ultrasonics, Volume 53, Issue 5, July 2013, Pages 962-972, http://dx.doi.org/10.1016/j.ultras.2012.12.012.

[8] M. Benaicha, O. Jalbaud, A.H. Alaoui, Y.Burtschell, Correlation between the mechanical behavior and the ultrasonic velocity of fiber-reinforced concrete, Construction and Building Materials, Volume 101, Part 1, 30 December 2015, Pages 702-709, http://dx.doi.org/10.1016/j.conbuildmat.2015.10.047.

[9] A. Boumiz, C. Vernet, F.Cohen Tenoudji, Mechanical properties of cement pastes and mortars at early ages, *Advanced Cement Based Materials*, Volume 3, Issue 3, 1996, Pages 94-106, http://dx.doi.org/10.1016/S1065-7355(96)90042-5.

[10] S. Popovics, J.L. Rose, J.S. Popovics, The behaviour of ultrasonic pulses in concrete, *Cement and Concrete Research*, Volume 20, Issue 2, 1990, Pages 259-270, http://dx.doi.org/10.1016/0008-8846(90)90079-D.

[11] K. Tharmaratnam, B.S. Tan, Attenuation of ultrasonic pulse in cement mortar, *Cement and Concrete Research*, Volume 20, Issue 3, May 1990, Pages 335-345, http://dx.doi.org/10.1016/0008-8846(90)90022-P.

[12] V. Garnier, G. Corneloup, J.M. Sprauel, J.C. Perfumo, Setting time study of roller compacted concrete by spectral analysis of transmitted ultrasonic signals, *NDT & E International*, Volume 28, Issue 1, February 1995, Pages 15-22, http://dx.doi.org/10.1016/0963-8695(94)00006-6.

[13] T.P. Philippidis, D.G. Aggelis, Experimental study of wave dispersion and attenuation in concrete, *Ultrasonics*, Volume 43, Issue 7, June 2005, Pages 584-595, http://dx.doi.org/10.1016/j.ultras.2004.12.001.

[14] S. Akçaözoğlu, K. Akçaözoğlu, C.D. Atiş, Thermal conductivity, compressive strength and ultrasonic wave velocity of cementitious composite containing waste PET lightweight aggregate (WPLA), *Composites Part B: Engineering*, Volume 45, Issue 1, February 2013, Pages 721-726, http://dx.doi.org/10.1016/j.compositesb.2012.09.012.

[15] B. Castagnéde, A. Moussatov, D. Lafarge, M. Saeid, Low frequency in situ metrology of absorption and dispersion of sound absorbing porous materials based on high power ultrasonic non-linearly demodulated waves, *Applied Acoustics*, Volume 69, Issue 7, July 2008, Pages 634-648, http://dx.doi.org/10.1016/j.apacoust.2007.01.006.

[16] T.P Philippidis, D.G Aggelis, An acoustic-ultrasonic approach for the determination of water-to-cement ratio in concrete, *Cement and Concrete Research*, Volume 33, Issue 4, April 2003, Pages 525-538, http://dx.doi.org/10.1016/S0008-8846(02)00999-7.

[17] D.E.W. Stone, B. Clarke, Ultrasonic attenuation as a measure of void content in carbon-fibre reinforced plastics, *Non-destructive Testing*, 1975, Pages 137–145.

[18] H. Jeong, D.K. Hsu, Experimental analysis of porosity-induced ultrasonic attenuation and velocity change in carbon composites, *Ultrasonics*, Volume 33, Issue 3, May 1995, Pages 195-203, http://dx.doi.org/10.1016/0041-624X(95)00023-V.

[19] L. Vergara, R. Miralles, J. Gosálbez, F.J. Juanes, L.G. Ullate, J.J. Anaya, M.G. Hernández, M.A.G. Izquierdo, NDE ultrasonic methods to characterise the porosity of mortar, *NDT & E International*, Volume 34, Issue 8, December 2001, Pages 557-562, http://dx.doi.org/10.1016/S0963-8695(01)00020-2.

[20] Z. Lafhaj, M. Goueygou, A. Djerbi, M. Kaczmarek, Correlation between porosity, permeability and ultrasonic parameters of mortar with variable water / cement ratio and water content, *Cement and Concrete Research*, Volume 36, Issue 4, April 2006, Pages 625-633, http://dx.doi.org/10.1016/j.cemconres.2005.11.009.

[21] P. Leclaire, L. Kelders, W. Lauriks, M. Melon, N. Brown, B. Castagnède, Determination of the viscous and thermal characteristic lengths of plastic foams by ultrasonic measurements in helium and air, *Journal of Applied Physics,* Volume 80, Issue 4, August 1996, Pages 2009-2012, http://dx.doi.org/10.1063/1.363817.

[22] I. Palomar, G. Barluenga, J. Puentes, Assessment by non-destructive testing of new mortar coatings for retrofitting the Architectural Heritage". *WIT Transactions on The Built Environment*, Volume 153, 2015, Pages 357-366, http://dx.doi.org/10.2495/STR150301.

[23] W.N. Reynolds, S.J. Wilkinson, The analysis of fibre-reinforced porous composite materials by the measurement of ultrasonic wave velocities, *Ultrasonics*, Volume 16, 1978, Pages 159–163, http://dx.doi.org/10.1016/0041-624X(78)90071-9

[24] M. Treiber, J. Kim, J. Qu, L.J. Jacobs, Effects of sand aggregate on ultrasonic attenuation in cement-based materials. *Materials and Structures,* Volume 43, Supplement 1, 2010, Pages 1-11, http://dx.doi.org/10.1617/s11527-010-9587-7.

[25] H. Hatanaka, Y. Kawano, N. Ido, M. Hato, M Tagami, Ultrasonic testing with advanced signal processing for concrete structures, *Nondestructive Testing and Evaluation*, Volume 20, Issue 2, June 2005, Pages 115-124.

[26] W. Punurai, J. Jarzynski, J. Qu, J. Kim, L.J. Jacobs, K.E. Kurtis, Characterization of multi-scale porosity in cement paste by advanced ultrasonic techniques, *Cement and Concrete Research*, Volume 37, Issue 1, January 2007, Pages 38-46, http://dx.doi.org/10.1016/j.cemconres.2006.09.016.

[27] M. Vasina, D.C. Hughes, K.V. Horoshenkov, L. Lapčík Jr., The acoustical properties of consolidated expanded clay granulates, *Applied Acoustics*, Volume 67, Issue 8, 2006, Pages 787–796 http://dx.doi.org/10.1016/j.apacoust.2005.08.003

[28] B. Rehder, K. Bahn, N. Neithalath, Fracture behavior of pervious concrete systems: the effects of pore structure and fibers, *Engineering Fracture Mechanics*, Volume 118, 2014, Pages 1-16, http://dx.doi.org/10.1016/j.engfracmech.2014.01.015.

[29] J. Carbajo, T.V. Esquerdo-Lloret, J. Ramis, A.V. Nadal-Gisbert, F.D. Denia, Acoustic modeling of perforated concrete using the dual porosity theory, *Applied Acoustics*, Volume 115, January 2017, Pages 150-157, http://dx.doi.org/10.1016/j.apacoust.2016.09.005.

Tables and figures

Table 1. Compositions of the lime-cement mortars (components in kg).

	D_a kg/m^3	REFC	FC15	FC30	A25	P50	P25	P25 FC30	P25 FPP	V50	V25
BL-II B-L 32.5 N	1256	214	214	214	214	214	214	214	214	214	214
CL-90-S	400	68	68	68	68	68	68	68	68	68	68
Cellulose fibres	40	-	0.8	1.6	-	-	-	1.6	-	-	-
Polypropylene fibres	910	-	-	-	-	-	-	-	0.81	-	-
Sand 2-3	1473	1502	1502	1502	1127	751	1127	1127	1127	751	1127
Expanded Clay	320	-	-	-	82	-	-	-	-	-	-
Perlite	150	-	-	-	-	77	38	38	38	-	-
Vermiculite	160	-	-	-	-	-	-	-	-	82	41
Water [a]	1000	140	140	140	160	260	220	220	225	300	270
D_{fresh} (kg/m^3)	-	1880	1790	1830	1630	1630	1790	1790	1770	1760	2030
Water/binder (w/b) [b]	-	0.56	0.56	0.56	0.61	0.96	0.83	0.83	0.85	1.10	1.01
Consistency (mm)	-	177	174	171	175	174	173	172	166	169	175

[a] Liquid water added.

[b] The total w/b includes LWA absorption water and the amount of water included in the components (sand humidity 1.27%).

Table 2. Mechanical and physical properties of lime-cement mortar samples.

	REFC	FC15	FC30	A25	P50	P25	P25 FC30	P25 FPP	V50	V25
f_{cm} (MPa) [a]	6.17	9.67	7.67	7.83	6.33	6.67	6.33	5.83	3.00	5.00
f_{ctm} (MPa) [a]	1.59	2.36	1.83	2.22	2.13	1.84	2.08	1.85	1.74	1.57
D (kg/m^3) [a]	1880	1830	1840	1590	1450	1580	1670	1550	1420	1650
P_O (%) [a]	17.83	16.42	16.22	17.01	26.41	21.85	21.83	20.64	29.16	24.79
C (kg/m^{2}min$^{0.5}$) [a]	0.53	0.65	0.55	0.50	1.08	0.88	1.07	0.83	1.30	1.48
P_V x 10^{-11} (kg/m s Pa) [a]	6.64	6.43	5.85	5.54	5.10	5.14	5.90	5.56	4.63	5.40
λ (W/mK) [b]	0.368	0.190	0.429	0.322	0.175	0.220	0.442	0.287	0.204	0.267
α_{NRC} (-) [b]	0.104	0.127	0.083	0.113	0.037	0.059	0.038	0.083	0.039	0.039

[a] The characterization in the hardened state was done at 28 days.

[b] The thermal and acoustic tests were carried out at 180 and 60 days, respectively.

Table 3. P-wave and S-wave UPV and attenuation results on lime-cement mortar samples at 2 years.

	REFC	FC15	FC30	A25	P50	P25	P25 FC30	P25 FPP	V50	V25
V_{P-54} (m/s)	2816	3013	2710	2855	2434	2440	2332	2378	1993	2200
V_{P-250} (m/s)	3007	3083	2899	2954	2410	2472	2486	2546	2180	2331
V_{s-250} (m/s)	1597	1697	1616	1535	1412	1375	1324	1434	1306	1421
M_{54} (GPa)	14.89	16.65	13.51	12.98	8.59	9.42	9.06	8.79	5.63	7.99
M (GPa)	16.98	17.43	15.47	13.89	8.42	9.67	10.30	10.08	6.73	8.97
G (GPa)	4.79	5.28	4.81	3.75	2.89	2.99	2.92	3.20	2.42	3.33
K (GPa)	10.60	10.39	9.06	8.89	4.57	5.68	6.40	5.82	3.51	4.53
E (GPa)	12.49	13.55	12.25	9.87	7.16	7.64	7.60	8.10	5.90	8.02
v (-)	0.30	0.28	0.27	0.31	0.24	0.28	0.30	0.27	0.22	0.20
AT_{54} (dB/mm)	0.169	0.198	0.194	0.261	0.241	0.238	0.273	0.202	0.185	0.205
AT_{250} (dB/mm)	0.124	0.120	0.108	0.127	0.108	0.103	0.175	0.157	0.098	0.087

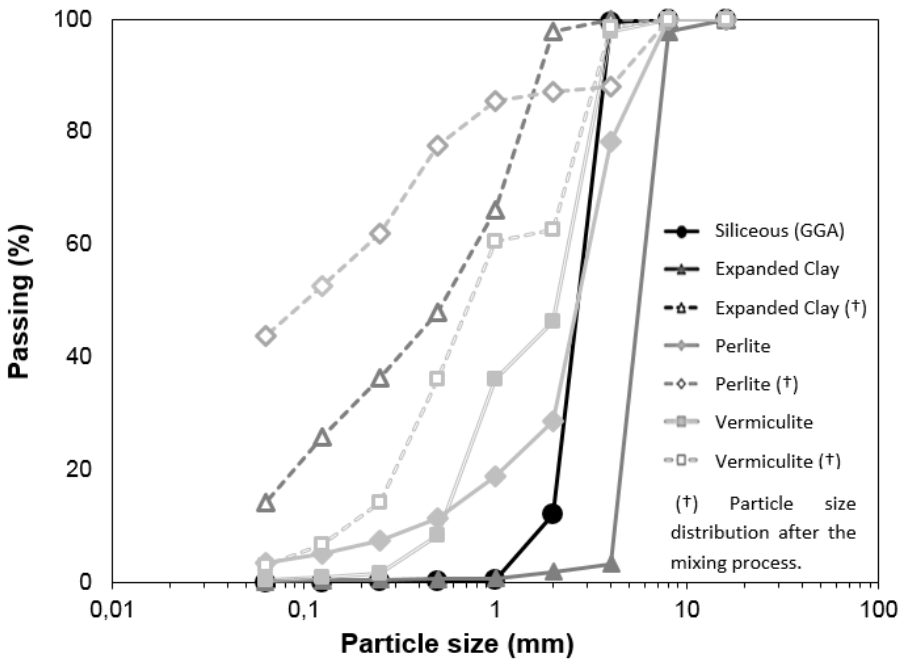

Fig. 1. Particle size distribution of gap-graded and lightweight aggregates.

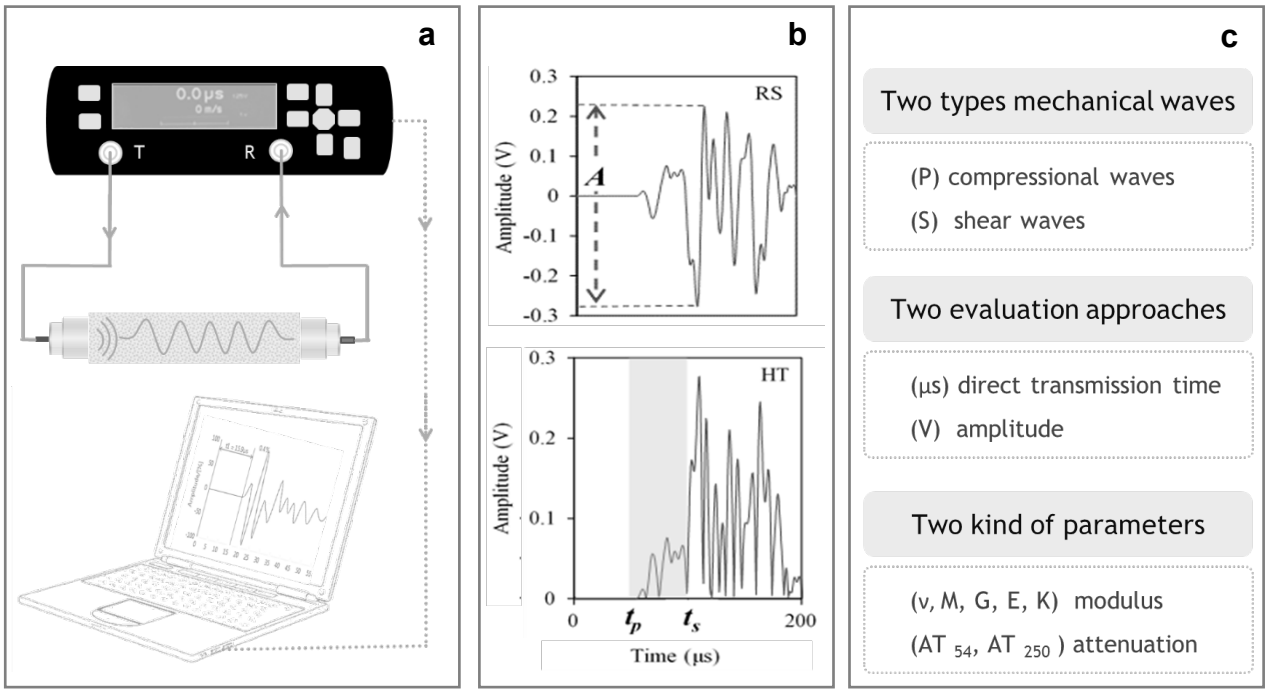

Fig. 2. Non-destructive testing (NDT) by ultrasonic pulses (US): a) experimental method; b) S-wave raw signal (250 kHz) through mortar in time (RS) and amplitude envelope (HT); and c) analytical method.

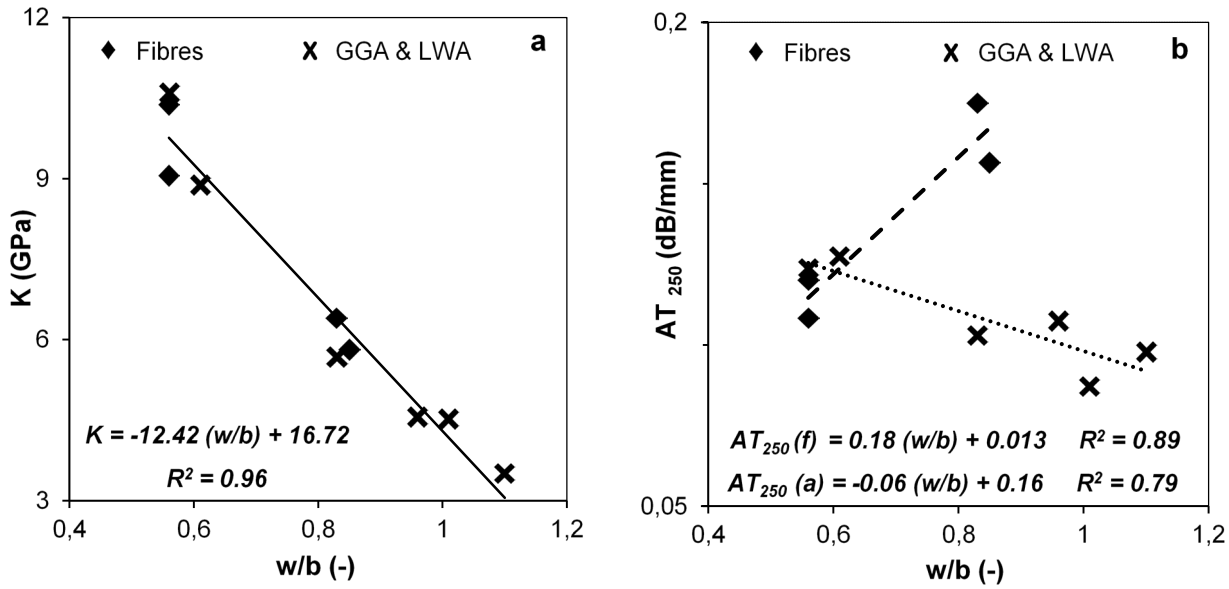

Fig. 3. Bulk modulus (K) and attenuation coefficient (AT_{250}) related to water to binder ratio (w/b).

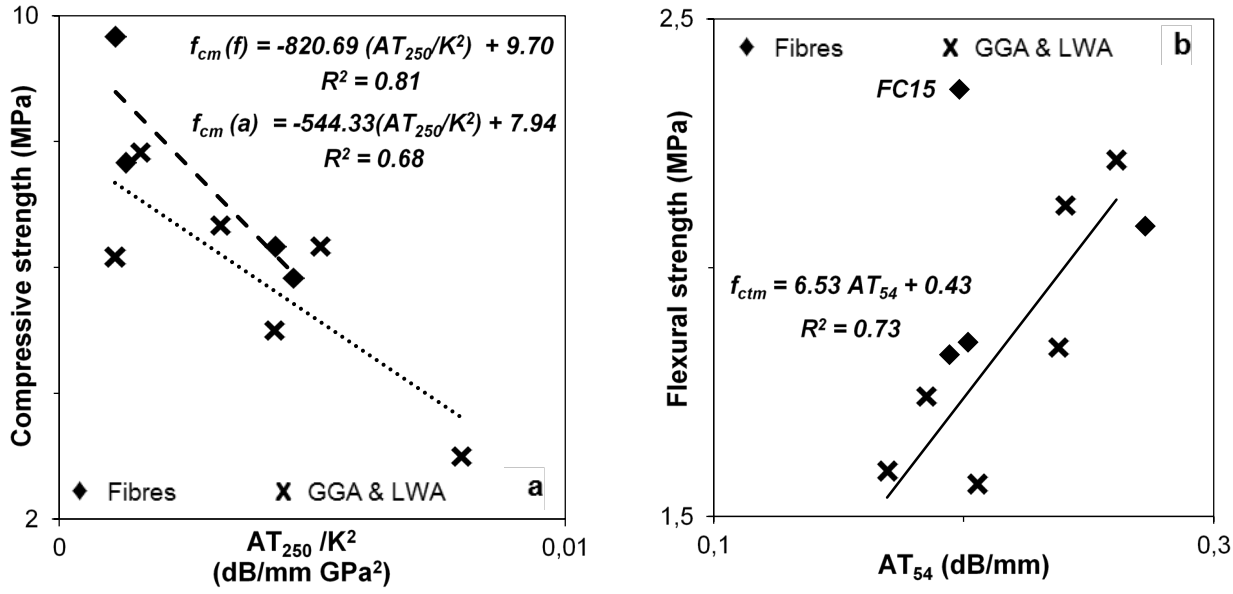

Fig. 4. Mechanical properties – compressive (f_{cm}) and flexural strength (f_{ctm}) – related to ultrasonic parameters (K, AT_{54} and AT_{250}).

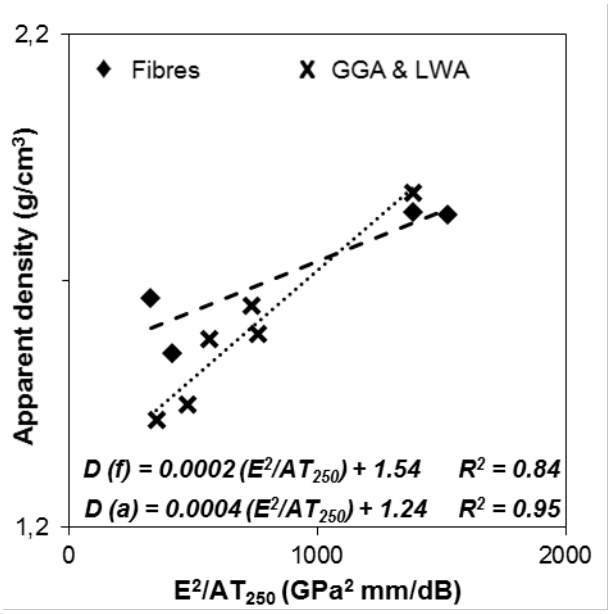

Fig. 5. Apparent density (D) – vs. ultrasonic parameters (E and AT_{250}).

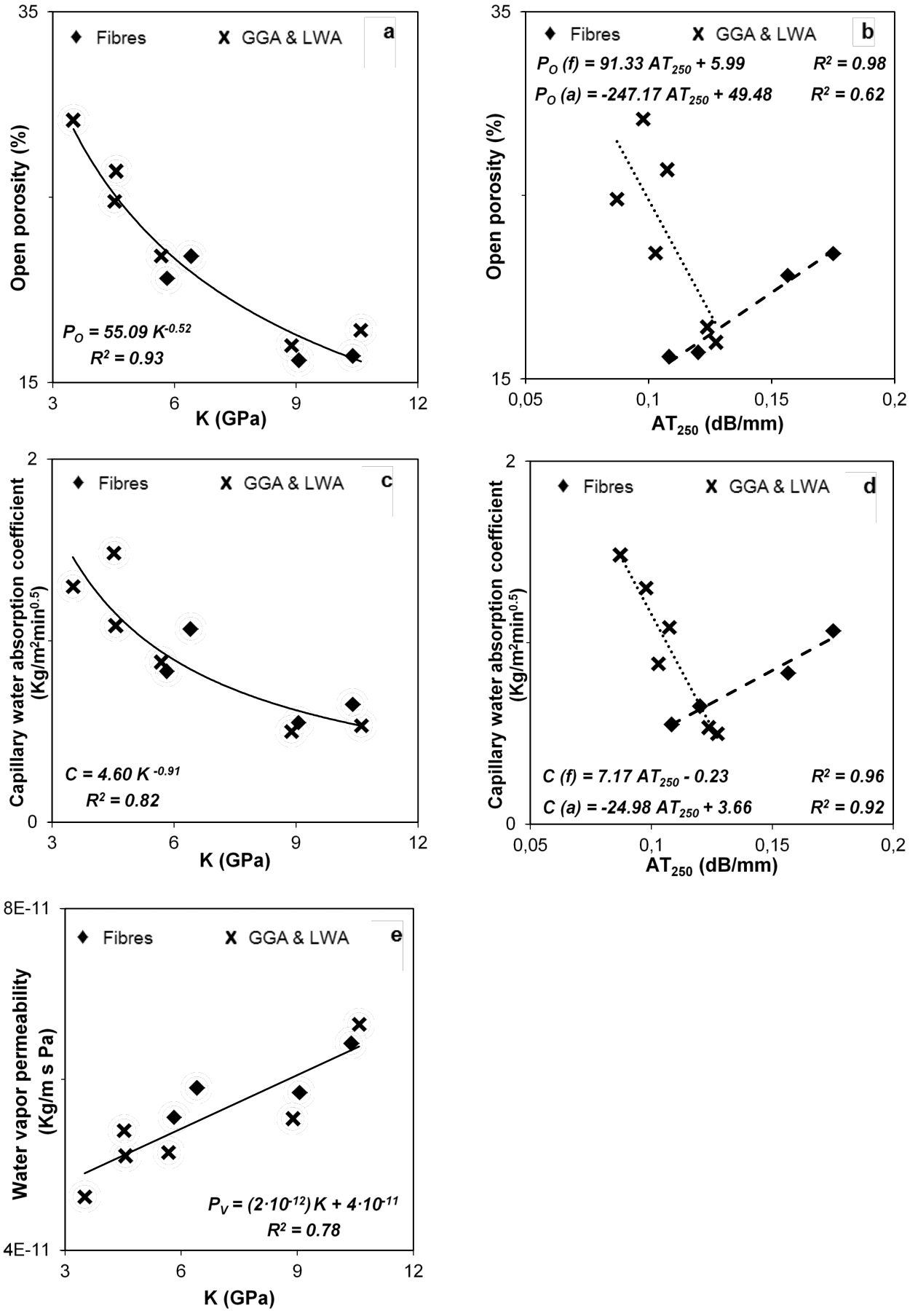

Fig. 6. Pore network: physical properties – open porosity (P_O), capillary water absorption coefficient (C) and water vapor permeability (P_V) – vs. ultrasonic parameters (K and AT_{250}).

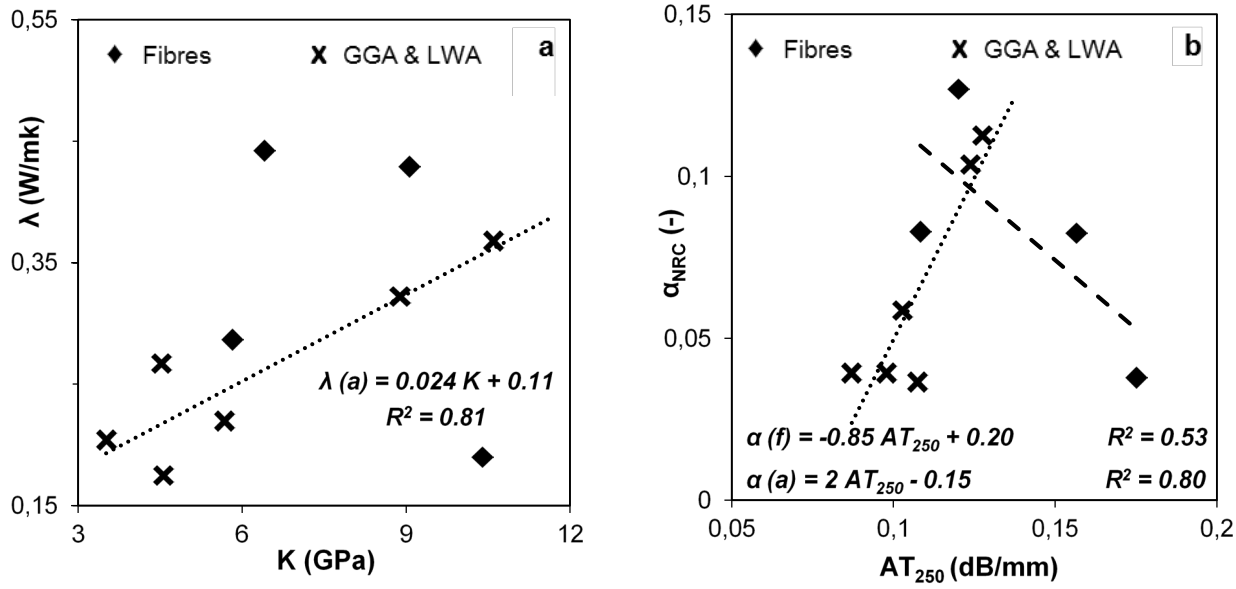

Fig. 7. Thermal and acoustic performance parameters– thermal conductivity (λ) and sound absorption coefficient (α_{NRC}) – correlated to ultrasonic parameters (K and AT_{250}).